Plasmonic Catalysis

DOI: 10.1002/anie.201301652

The Synthesis of Size- and Color-Controlled Silver Nanoparticles by Using Microwave Heating and their Enhanced Catalytic Activity by Localized Surface Plasmon Resonance**

*Kojirou Fuku, Ryunosuke Hayashi, Shuhei Takakura, Takashi Kamegawa, Kohsuke Mori, and Hiromi Yamashita**

Clean energy production, organic transformations through energy-conserving processes, and efficient disposal of harmful waste are desirable from the point of view of reducing environmental problems, such as global warming and air and water pollution. Supported metallic nanoparticle (NP) catalysts are widely recognized as an important class of industrial catalysts that resolve the above issues.[1] Significant efforts have recently been devoted to achieving NPs with precise architectures, in which the size, composition and morphology are controlled; changes to these parameters enable the catalytic activity and selectivity of such catalysts to be tuned. The development of synthetic methods to provide NPs suitable for particular catalytic reactions is important.[2]

Metallic NPs, such as Au, Ag, and Cu, can absorb visible and infrared light in particular regions owing to localized surface plasmon resonance (LSPR).[3] In simple terms, LSPR is made up of collective oscillations of free electrons in metal NPs driven by the electromagnetic field of incident light.[4] This unique characteristic has given rise to a new approach to the fabrication of visible-light-responsive photocatalysts, known as plasmonic photocatalysts; this approach involves the deposition of metallic NPs onto suitable semiconductors.[5] It has been proposed that for Au/TiO_2 catalysts, at an excitation wavelength corresponding to the LSPR of Au, the Au NPs absorb photons and transfer photogenerated electrons into the TiO_2 conduction band.[5b,c]

The charge density of such plasmonic NPs is partially localized on the surface, and this localization is increased by charge separation derived from the LSPR effect, in the absence of a semiconductor to act as an electron acceptor.[4] As catalysis primarily occurs on the metallic surface, we anticipated that the catalytic performance of such plasmonic NPs could be significantly enhanced by the use of inert silica as a support material because of the localized surface charge density induced by the LSPR effect. More interestingly, the color of the plasmonic NPs can be systematically tuned, owing to changes in the LSPR absorption wavelength, by varying the size and morphology of the particles.[6] However, the application of plasmonic NPs with unique characteristics owing to LSPR, such as localization of surface charge density and color control, as catalysts have not yet been investigated.

Herein, we describe a new method for the synthesis of Ag NPs, the color of which can be altered by changing the size and morphology: this method involves microwave heating and the use of SBA-15 mesoporous silica material. We also demonstrated that the localized surface charge of these Ag NPs results in them having enhanced catalytic activity under visible light irradiation owing to LSPR, compared to Ag NPs obtained by pure thermal processes. As expected, the enhancement was dependent on the Ag NPs used. The plasmonic metal NP catalysts could be designed with the optimal size and color for target reactions and light sources, thus making it possible to achieve the maximum catalytic activity in various light environments.

SBA-15 mesoporous silica was prepared according to a previously reported procedure.[7] The diffraction pattern obtained by low-angle XRD measurement for SBA-15 exhibited two peaks at around 1.0–2.0°, corresponding to a hexagonal structure, thus indicating the formation of an ordered mesoporous structure (see the Supporting Information, Figure S1).[8] The N_2 adsorption–desorption measurements showed that SBA-15 possessed a high specific surface area and a mesopore structure of 9.2 nm (see the Supporting Information, Table S1).[8] Three types of Ag NPs were prepared on SBA-15 by microwave-assisted alcohol reduction with varying irradiation times (3 or 5 min) in the presence or absence of sodium laurate (Lau) as a surface-modifying ligand (Ag: 1 wt%): **1** (3 min, with sodium laurate), **2** (3 min, without sodium laurate), and **3** (5 min, without sodium laurate). Microwave induction heating has recently attracted considerable attention as a potential method for the preparation of monodispersed inorganic materials because energy-efficient microwave irradiation results in internal, rapid, and uniform heating; this method can also be used for the simple and energy-saving preparation of inorganic nanostructured materials.[9] Although many studies of the preparation of metallic colloids and clusters have been reported, there are

[*] K. Fuku, R. Hayashi, S. Takakura, Dr. T. Kamegawa, Dr. K. Mori, Prof. Dr. H. Yamashita
Graduate School of Engineering, Osaka University
1-2 Yamadaoka, Suita, Osaka 565-0871 (Japan)
E-mail: yamashita@mat.eng.osaka-u.ac.jp
Homepage: http://www.mat.eng.osaka-u.ac.jp/msp1/Englishmenu.htm
Dr. K. Mori, Prof. Dr. H. Yamashita
Unit of Elements Strategy Initiative for Catalysts & Batteries
Kyoto University, ESICB, Kyoto Univ. (Japan)

[**] The authors appreciate assistance from Dr. Eiji Taguchi and Prof. Hidehiro Yasuda at the Research Center for Ultra-High Voltage Electron Microscopy, Osaka University for TEM measurements. The X-ray absorption experiments were performed at the Spring-8, Harima (Japan).

Supporting information for this article is available on the WWW under http://dx.doi.org/10.1002/anie.201301652.

only a few examples of the microwave-assisted synthesis of size-controlled metallic NPs on supports.[10]

As shown in the TEM images in Figure 1, SBA-15 exhibited a well-ordered mesoporous channel structure, which was confirmed by the low-angle XRD pattern and N_2

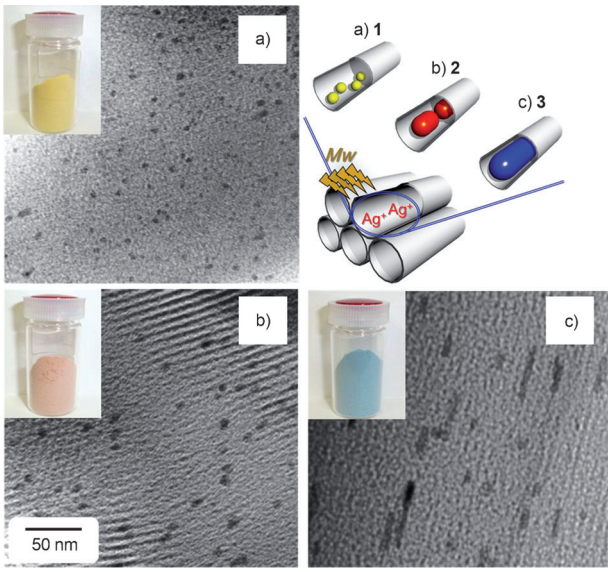

Figure 1. TEM images and photographs of samples (insets) of Ag/SBA-15: a) **1**, b) **2**, and c) **3**.

adsorption–desorption measurements. Ag NPs were successfully deposited on SBA-15. Spherical Ag NPs with a mean diameter of approximately 4 nm and a narrow size distribution were formed within the mesoporous channels of SBA-15 in **1** (Figure 1a), which was prepared by microwave irradiation for 3 min in the presence of Lau. In contrast, in **2** (Figure 1b) and **3** (Figure 1c), which were prepared in the absence of surface-modifying ligands under microwave irradiation for 3 and 5 min, respectively, Ag nanorods were formed parallel to the SBA-15 mesopores. The aspect ratio of the Ag nanorods increased markedly with increasing microwave irradiation time. The average diameter of these Ag nanorods was approximately 9 nm, which was in close agreement with the pore size of SBA-15. The obtained Ag NPs were also characterized by Ag K-edge XAFS spectra (see the Supporting Information, Figure S2).[8] The XANES spectra of all samples were similar to that of Ag foil, suggesting the presence of Ag in the metallic state. In the Fourier transforms of the Ag K-edge EXAFS spectra, all samples exhibited a peak at approximately 2.7 Å, which corresponds to the contiguous Ag–Ag bond in the metallic nanoparticles. The peak intensity decreased in the order of **3** > **2** > **1**; this trend is due to the smaller size of the Ag particles. The order of peak intensity was in close agreement with the order of Ag particle size observed by TEM (Figure 1). In addition, the colors of these samples were yellow (**1**), red (**2**), and blue (**3**), which reflected the UV/Vis spectra. All of the Ag NPs exhibited different UV/Vis absorption characteristics, derived from the corresponding Ag LSPR (see the Supporting Information, Figure S3).[8] The intensity and wavelength of LSPR absorption depended on the size, morphology, and aspect ratio of the Ag NPs; a red shift in the LSPR absorption was observed as the size and aspect ratio of the Ag nanoparticles increased.[6a] For comparison, Ag deposition on SBA-15 was also performed by heating by using a conventional oil bath at 413 K with stirring. However, Ag NPs with a variety of morphologies, including spheres and nanorods, and wide size distributions were formed in the presence of Lau, whereas hardly any Ag NPs were formed in the absence of Lau (see the Supporting Information, Figures S4 and S5).[8] It was concluded that the SBA-15 mesopores and microwave heating were required to attain rapid production and uniform growth of the Ag nuclei.

To investigate the effect of the size and color of the Ag NPs on their catalytic performance, H_2 production from ammonia borane (NH_3BH_3) was studied as the model reaction. NH_3BH_3, which produces only H_2 as a gas product and possesses high H_2 storage capacity (19.6 wt%), has attracted attention as a promising next-generation hydrogen storage material. Recently, the use of various NPs, such as Au, Pd, Ru, Cu, Ni, Fe, and Au/Co, for the efficient production of H_2 from NH_3BH_3 has been widely investigated and H_2 has been stoichiometrically produced in a 3:1 (H_2/NH_3BH_3) molar ratio, as shown in Equation (1).[11] Noble metal catalysts with superior catalytic activity under mild conditions are particularly desirable as they are expected to have widespread applications.

$$NH_3BH_3 + 2\,H_2O \rightarrow NH_4^+ + BO_2^- + 3\,H_2 \qquad (1)$$

Initially, H_2 production from aqueous NH_3BH_3 (20 μmol) was performed under an Ar atmosphere at room temperature (25 °C) in the dark to evaluate the catalytic performance of size-controlled Ag NPs on SBA-15 (see the Supporting Information, Figure S6).[8] No catalytic activity was observed in the control experiment (without catalyst). In contrast, all of the Ag/SBA-15 catalysts exhibited H_2 production activity. The catalytic activity depended on the size of the Ag NP: the smallest Ag NP, **1** (Figure S6a), was a more efficient catalyst than **2** (Figure S6b) and **3** (Figure S6c). The H_2 production reaction was complete (ca. 60 μmol) within a short reaction time when the smallest Ag NPs were used. These results suggest that catalytic H_2 production from NH_3BH_3 in the dark occurred on the exposed Ag atoms on the surface of the NPs. It is apparent from the results of previously reported catalyst systems that the TOF values achieved with Ag/SBA-15 is 0.2 h^{-1}, which is higher than those reported for other catalyst systems, such as Cu/γ-Al_2O_3 (0.09 min^{-1}),[11d] metallic Fe crystallites (0.05 min^{-1}),[11e] and Ni/SiO_2 (0.16 min^{-1}).[11f]

To achieve maximum efficiency of the Ag NP catalysts, the effect of the Ag LSPR on H_2 production activity was investigated under light irradiation. Figure 2 shows the time course of the initial H_2 production on Ag/SBA-15 in the dark or under light irradiation (wavelength $\lambda > 420$ nm, 320 mW cm^{-2}). The catalytic performance of all Ag NPs was enhanced with light irradiation. Interestingly, the rate of H_2 production was significantly dependent on the color of the Ag NPs, and increased in the following order: **1** (29%) < **2** (66%) < **3** (124%). This trend matched the corresponding

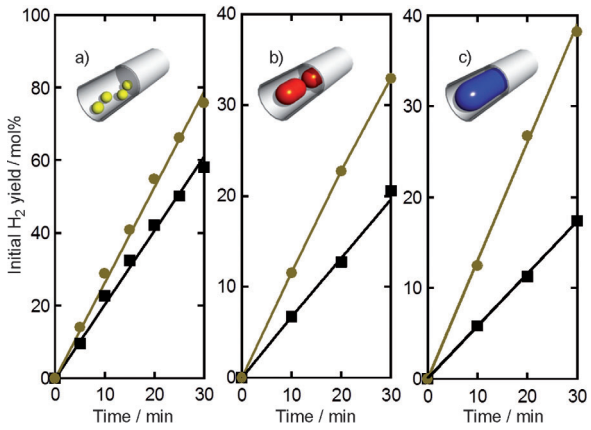

Figure 2. Time courses of initial H_2 production in the presence of Ag/SBA-15 in the dark (black ■) or under light irradiation at wavelength $\lambda > 420$ nm (gold ●): a) **1**, b) **2**, and c) **3**.

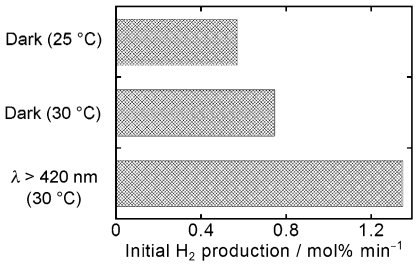

Figure 3. Comparison of initial H_2 production on Ag/SBA-15 **3** in the dark (25 or 30 °C) or under light irradiation ($\lambda > 420$ nm).

trend in Ag LSPR absorption intensity at wavelengths of more than 420 nm. The off/on effect of this light irradiation was also investigated and Ag/SBA-15 **3** exhibited the highest increase in catalytic activity (see the Supporting Information, Figure S7).[8] After reaction in the dark for 15 min (light off), the catalytic activity was significantly enhanced by light irradiation (light on). It should be noted that the slope of activity under light irradiation after reaction in the dark for 15 min was almost the same as that of activity under light irradiation after no reaction in the dark (from 0 min). To the best of our knowledge, this is the first demonstration for the enhancement of catalytic activity of color-controlled Ag NPs by the assistance of LSPR. Moreover, the catalyst could be completely recovered without the leaching of active components. Recovered Ag/SBA-15 **1** retained its original catalytic activity both under light irradiation and in the dark (Figure S8),[8] thus suggesting that this catalytic reaction proceeded on the Ag NPs deposited on the silica surface, but not with detached Ag species.

Because light irradiation from a Xe lamp at $\lambda > 420$ nm contains not only visible light but also infrared light, the above enhancement of catalytic activity under light irradiation could simply be due to heating by the infrared light. In fact, the temperature of the suspension of Ag/SBA-15 **3** increased slightly (about 5 °C) under light irradiation, because the Ag nanorods exhibit wide light absorption by LSPR over the infrared region (see the Supporting Information, Figure S3).[8] In an effort to exclude the thermal effect of infrared light, the thermal reaction at 30 °C was performed in the dark with Ag/SBA-15 **3**. The initial H_2 production in the dark at 30 °C was 0.74 mol % min^{-1}, which was slightly higher than the production (0.57 mol % min^{-1}) in the dark at room temperature (25 °C), but was significantly lower than the production (1.35 mol % min^{-1}) under light irradiation (Figure 3). Also, the plasmonic heating of Ag NPs derived from plasma oscillation by LSPR, as previously reported by Christopher et al., can be calculated as shown in Equation (2).[12]

$$T = T_\infty + \frac{I_0 K_{abs} r_0}{6k_\infty} \quad (2)$$

This equation can be used as a function of light intensity (I_0), absorption efficiency (K_{abs}), the diameter of metallic NP (r_0), the thermal conductivity of the surrounding medium (k_∞) and heating temperature (T_∞). By using the experimental values $I_0 = 320$ mW cm^{-2}, $r_0 = 4$–50 nm, $T_\infty = 298$ K, and the values calculated by Christopher et al. ($K_{abs} = 3$, $k_\infty = 40$ mW m^{-1} K^{-1}), the increase in temperature due to the plasmonic heating in our reaction system was determined to be less than 0.002 K. These results suggest that the enhanced catalytic performance originated primarily owing to Ag LSPR under irradiation, and the contribution from heating was negligible.

The effect of Ag LSPR on catalytic performance was also investigated by using a red LED lamp with a maximum wavelength $\lambda_{max} = 650$ nm (25 mW cm^{-2}) (see the Supporting Information, Figure S9).[8] Although this red LED light contains only visible light and no infrared light, a similar enhancement of the catalytic performance was obtained for all Ag NPs. The rate of enhancement of catalytic performance depended significantly on the type of Ag NP and increased in the order **1** < **2** < **3**, which was consistent with the order of the Kubelka–Munk (KM) function intensity derived from Ag -LSPR at irradiation wavelength ($\lambda_{max} = 650$ nm) calculated from UV/Vis measurements (see the Supporting Information, Figure S3).[8] There was no increase in the temperature of these Ag/SBA-15 suspensions under this red light irradiation. In addition, the wavelength dependence of the enhancement of the catalytic performance of Ag/SBA-15 having various colors was investigated by using monochromatic light ($\lambda =$ 400, 440 and 460 nm, 6 mW cm^{-2}). As shown in Figure 4, the increasing rates of catalytic performance with light intensities were highly consistent with the LSPR absorption of these Ag NPs. Notably, the increases in catalytic performance under light irradiation were entirely dependent on the particle color derived from Ag LSPR. This wavelength dependence also suggests that the increase in catalytic performance was derived from the Ag LSPR, and that maximum efficiency can be attained by using Ag NPs of appropriate colors for the light environment.

The mechanism for catalytic H_2 production from NH_3BH_3 has been reported for both heterogeneous and homogeneous catalysis.[11d,13] In the case of catalysis by metallic NPs, a plausible mechanism involves adsorption of NH_3BH_3 onto the metallic NPs to form an activated complex, which is the rate-determining step, followed by H_2 production through attack by a H_2O molecule. In homogeneous catalysis using

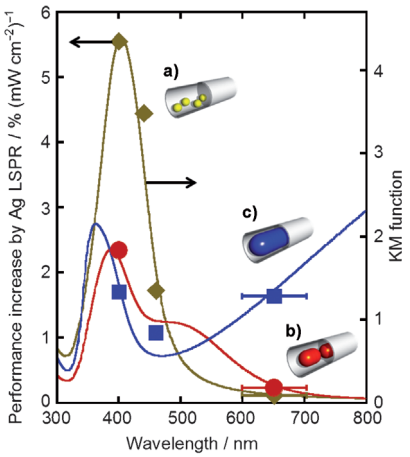

Figure 4. Wavelength dependence of the enhancement of catalytic performance of Ag/SBA-15: a) **1**, b) **2**, and c) **3** under irradiation by monochromatic light ($\lambda = 400$, 440 and 460 nm) and red LED light ($\lambda_{max} = 650$ nm).

metal halides, high H_2 production activity is obtained by the addition of a Lewis acid such as Co^{2+} ions to the reaction mixture; this increased activity can be simply explained by cooperative activation of Lewis basic NH_3BH_3 with the assistance of the electron-deficient Lewis acid sites. Thus, we predict that the enhancement of the catalytic activity for H_2 production from NH_3BH_3 by Ag LSPR is due to the increasing surface charge density of the Ag nanoparticles derived from the charge separation effect under light irradiation.

To confirm that the enhancement in the H_2 production is due to Ag LSPR, $NaHCO_3$ (100 μmol) was added as a positive charge scavenger to a suspension of Ag/SBA-15 **3** under light irradiation by a red LED lamp ($\lambda_{max} = 650$ nm) and a Xe lamp through a glass filter ($\lambda > 420$ nm). HCO_3^- adsorbs highly onto the Ag NP surface, where it can interact with the generated H^+ (positive charge) on the Ag NPs.[5d] The enhancement in the H_2 production was decreased significantly by the presence of $NaHCO_3$ (see the Supporting Information, Figure S10).[8] The inhibition ratio of catalytic activity in the presence of HCO_3^- under light irradiation is significantly higher than that observed for the reaction in the dark (see the Supporting Information, Figure S11).[8] Ag NPs produce cyclical charge separation by wavelength-dependent collective oscillations of free electrons, resulting in the formation of a transitory deficient site of electron population (plasmon).[4] It was concluded that HCO_3^- adsorbed on the Ag NPs reacted with the positive charge resulting from charge separation derived from the Ag LSPR plasma oscillation, and activation of the NH_3BH_3 was markedly suppressed.

In summary, size- and color-controlled Ag NPs were successfully synthesized within the mesopore structure of SBA-15 by microwave-assisted alcohol reduction. The Ag NPs exhibited different catalytic activities when used for H_2 production from NH_3BH_3 in the dark; higher catalytic performance was observed for smaller Ag NPs. In addition, the catalytic performance was enhanced by light irradiation. It should be noted that the order of increasing catalytic performance was in close agreement with the order of absorption intensity of the irradiated light by Ag LSPR. From the results of experiments to investigate the thermal effect, wavelength dependence, and the effect of a charge scavenger, it was concluded that the H_2 production reaction was promoted by the positive charge generated by charge separation due to Ag LSPR. This study constitutes a promising approach to the preparation of highly ordered metallic NPs and the enhancement of catalytic performance under mild conditions, and we expect that this strategy can be extended to the preparation of other metallic NPs as well as the exploitation of highly efficient catalytic processes.

Experimental Section

Materials: Tetraethoxysilane (TEOS), hydrochloric acid, 1-hexanol, acetone, $AgNO_3$, and sodium laurate (Lau) were purchased from Nacalai Tesque Inc. Triblock copolymer P123 and ammonia borane (NH_3BH_3) were purchased from Sigma–Aldrich Co. All chemicals were used as received without further purification.

Preparation of Ag nanoparticles on SBA-15 mesoporous silica: SBA-15 was prepared according to a previous report, involving the sol–gel method using TEOS as a silica source and triblock copolymer P123 as a template.[7] Typically, a 1-hexanol suspension of SBA-15 powder (0.396 g), an aqueous solution of $AgNO_3$ (0.037 mmol), and Lau (10 mg), as surface-modifying ligand for Ag, were irradiated by microwave (500 W, 2450 ± 30 MHz) under an Ar atmosphere. After filtration and washing with acetone and distilled water, the resulting powder was dried at 343 K overnight under air. Size control of the Ag nanoparticles was achieved by varying the irradiation time (3 or 5 min) and in the presence or absence of Lau, resulting in the formation of 1 wt% Ag nanoparticles supported on SBA-15 (Ag/SBA-15) of three types (**1**, **2**, and **3**).

Catalytic activity test: H_2 production from NH_3BH_3: H_2 production from NH_3BH_3 was carried out in an aqueous suspension of various Ag/SBA-15 powders. The Ag/SBA-15 powder (20 mg) was suspended in distilled water (5 mL) in a test tube. After bubbling Ar through the mixture, NH_3BH_3 (20 μmol) was injected into the mixture through a rubber septum. The test tube was photoirradiated at a wavelength $\lambda > 420$ nm (320 mW cm^{-2}), by monochromatic light ($\lambda = 400$, 440 and 460 nm, 6 mW cm^{-2}) from a 500 W Xe lamp through a glass filter or a band-pass filter, or at a maximal wavelength $\lambda_{max} =$ 650 nm (25 mW cm^{-2}) by a red LED lamp, with magnetic stirring at room temperature (25 °C). The amount of H_2 in the gas phase was measured by using a Shimadzu GC-8A gas chromatograph equipped with a MS-5A column.

Received: February 26, 2013
Revised: April 10, 2013
Published online: June 6, 2013

Keywords: mesoporous silica · microwave chemistry · nanoparticles · silver · surface plasmon resonance

[1] a) J. M. Thomas, R. Raja, D. W. Lewis, *Angew. Chem.* **2005**, *117*, 6614; *Angew. Chem. Int. Ed.* **2005**, *44*, 6456; b) J. Sun, H. Liu, *Green Chem.* **2011**, *13*, 135; c) G. Novell-Leruth, A. Valcárcel, J. Pérez-Ramírez, J. M. Ricart, *J. Phys. Chem. C* **2007**, *111*, 860; d) Z. Tang, S. Shen, J. Zhuang, X. Wang, *Angew. Chem.* **2010**, *122*, 4707; *Angew. Chem. Int. Ed.* **2010**, *49*, 4603; e) K. Fuku, K. Hashimoto, H. Kominami, *Chem. Commun.* **2010**, *46*, 5118; f) K. Fuku, K. Hashimoto, H. Kominami, *Catal. Sci. Technol.* **2011**, *1*, 586; g) K. Fuku, T. Sakano, T. Kamegawa, K. Mori, H.

Yamashita, *J. Mater. Chem.* **2012**, *22*, 16243; h) Y. Kuwahara, K. Nishizawa, T. Nakajima, T. Kamegawa, K. Mori, H. Yamashita, *J. Am. Chem. Soc.* **2011**, *133*, 12462; i) Y. Kuwahara, D. Y. Kang, J. R. Copeland, N. A. Brunelli, S. A. Didas, P. Bollini, C. Sievers, T. Kamegawa, H. Yamashita, C. W. Jones, *J. Am. Chem. Soc.* **2012**, *134*, 10757.

[2] a) H. Tsunoyama, N. Ichikuni, H. Sakurai, T. Tsukuda, *J. Am. Chem. Soc.* **2009**, *131*, 7086; b) T. Fujitani, I. Nakamura, T. Akita, M. Okumura, M. Haruta, *Angew. Chem.* **2009**, *121*, 9679; *Angew. Chem. Int. Ed.* **2009**, *48*, 9515; c) Y. M. Chen, Z. X. Liang, F. Yang, Y. W. Liu, S. L. Chen, *J. Phys. Chem. C* **2011**, *115*, 24073.

[3] a) K. Mori, M. Kawashima, M. Che, H. Yamashita, *Angew. Chem.* **2010**, *122*, 8780; *Angew. Chem. Int. Ed.* **2010**, *49*, 8598; b) J. L. Duan, T. W. Cornelius, J. Liu, S. Karim, H. J. Yao, O. Picht, M. Rauber, S. Muller, R. Neumann, *J. Phys. Chem. C* **2009**, *113*, 13583.

[4] a) M. A. Noginov, G. Zhu, A. M. Belgrave, R. Bakker, V. M. Shalaev, E. E. Narimanov, S. Stout, E. Herz, T. Suteewong, U. Wiesner, *Nature* **2009**, *460*, 1110; b) J. N. Anker, W. P. Hall, O. Lyandres, N. C. Shah, J. Zhao, R. P. Van Duyne, *Nat. Mater.* **2008**, *7*, 442.

[5] a) S. K. Cushing, J. T. Li, F. K. Meng, T. R. Senty, S. Suri, M. J. Zhi, M. Li, A. D. Bristow, N. Q. Wu, *J. Am. Chem. Soc.* **2012**, *134*, 15033; b) C. Gomes Silva, R. Juarez, T. Marino, R. Molinari, H. Garcia, *J. Am. Chem. Soc.* **2011**, *133*, 595; c) A. Tanaka, S. Sakaguchi, K. Hashimoto, H. Kominami, *Catal. Sci. Technol.* **2012**, *2*, 907; d) C. Hu, T. W. Peng, X. X. Hu, Y. L. Nie, X. F. Zhou, J. H. Qu, H. He, *J. Am. Chem. Soc.* **2010**, *132*, 857.

[6] a) Y. W. Xie, S. Quinlivan, T. Asefa, *J. Phys. Chem. C* **2008**, *112*, 9996; b) T. M. D. Dang, T. T. T. Le, E. Fribourg-Blanc, M. C. Dang, *Adv. Nat. Sci. Nanosci. Nanotechnol.* **2011**, *2*, 1; c) A. Moores, F. Goettmann, *New J. Chem.* **2006**, *30*, 1121.

[7] K. Mori, K. Watanabe, M. Kawashima, M. Che, H. Yamashita, *J. Phys. Chem. C* **2011**, *115*, 1044.

[8] See the Supporting Information for details.

[9] a) J. A. Gerbec, D. Magana, A. Washington, G. F. Strouse, *J. Am. Chem. Soc.* **2005**, *127*, 15791; b) K. Fuku, T. Kamegawa, K. Mori, H. Yamashita, *Chem. Asian J.* **2012**, *7*, 1366.

[10] a) M. Tsuji, M. Hashimoto, Y. Nishizawa, M. Kubokawa, T. Tsuji, *Chem. Eur. J.* **2005**, *11*, 440; b) T. Nakamura, Y. Tsukahara, T. Sakata, H. Mori, Y. Kanbe, H. Bessho, Y. Wada, *Bull. Chem. Soc. Jpn.* **2007**, *80*, 224; c) S. Kundu, K. Wang, H. Liang, *J. Phys. Chem. C* **2009**, *113*, 134; d) G. Glaspell, L. Fuoco, M. S. El-Shall, *J. Phys. Chem. B* **2005**, *109*, 17350.

[11] a) H. L. Jiang, S. K. Singh, J. M. Yan, X. B. Zhang, Q. Xu, *ChemSusChem* **2010**, *3*, 541; b) G. Z. Chen, S. Desinan, R. Rosei, F. Rosei, D. L. Ma, *Chem. Eur. J.* **2012**, *18*, 7925; c) J. M. Yan, X. B. Zhang, T. Akita, M. Haruta, Q. Xu, *J. Am. Chem. Soc.* **2010**, *132*, 5326; d) Q. Xu, M. Chandra, *J. Power Sources* **2006**, *163*, 364; e) J.-M. Yan, X.-B. Zhang, S. Han, H. Shioyama, Q. Xu, *Angew. Chem.* **2008**, *120*, 2319; *Angew. Chem. Int. Ed.* **2008**, *47*, 2287; f) T. Umegaki, J.-M. Yan, X.-B. Zhang, H. Shioyama, N. Kuriyama, Q. Xu, *J. Power Sources* **2009**, *191*, 209.

[12] P. Christopher, H. L. Xin, S. Linic, *Nat. Chem.* **2011**, *3*, 467.

[13] a) R. Chiriac, F. Toche, U. B. Demirci, O. Krol, P. Miele, *Int. J. Hydrogen Energy* **2011**, *36*, 12955.

